Erosion Wear Response of Pineapple Leaf Fiber (PALF) Reinforced Vinylester Composites Filled With Redmud: an Alumina plant waste

[1]Yogesh M, [2]Dr. Hari Rao A N
[1]Associate Professor, [2]Professor
[1]Departmnet of Mechanical Engineering,
[1]GSSS Institute of Engineering and Technology of for Women, Mysuru, India
[2]Sri Jayachamarajendra College of Engineering, Mysuru, India

Abstract: - Natural fiber based composites are under intensive study due to their eco friendly nature and peculiar properties. The advantage of natural fibers is their continuous supply, easy and safe handling, and biodegradable nature. Natural fibers exhibit admirable physical and mechanical properties. Pineapple leave fiber (PALF) is one of the natural fiber abundantly available wastes materials in India and has not been studied yet. This research work is carried out a possibility that the incorporation of both particulate filler and fibers in polymer could provide a synergism in terms of improved properties. In view of this, the present research work is undertaken the fabrication of a set of Pineapple leaf fiber (PALF) reinforced Vinylester composites filled with Redmud an alumina plant waste product as the particulate filler. These results are compared with those of a similar set of Glass fiber reinforced Vinylester composites filled with same particulate filler. It also attempts to study the solid particle erosion wear response of these composites under multiple impact condition. The methodology based on Taguchi's experimental design approach is employed to make a parametric analysis of erosion wear process. This systematic experimentation has led to determination of significant process parameters and material variables that predominantly influence the wear rate of the particulate filled composites reinforced with pineapple leaf fiber. The significant control factors predominantly influencing the wear rate are identified. The filler content in the composites, the impingement angle and erodent temperature are found to have substantial influence in determining the rate of material loss from the composite surface due to erosion.

Keywords: - Natural fiber, Pineapple leaf fiber, particulate filler, Red mud, Taguchi experimental design, erosion wear

I. INTRODUCTION

Over the past few decades, it is found that polymers have replaced many of the conventional metals/materials in various applications. This is possible because of the advantages such as ease of processing, productivity, cost reduction etc. offered by polymers over conventional materials. In most of these applications, the properties of polymers are modified by using fibers to suit the high strength/high modulus requirements. All synthetic polymers (Thermoplastics, Thermoset and Elastomers) can be used as matrices in PMCs. As far as the reinforcement is concerned, extensive use has been made of inorganic man-made fibers such as glass and organic fibers such as carbon and aramid. As all these reinforcing fibers are expensive, various fibers like cellulose, wool, silk etc. abundantly available in natures are also used in composites. Cellulosic fibers like henequen, sisal, coconut fiber (coir), jute, palm, bamboo, Pineapple leaves fiber (PALF) and wood, in their natural conditions and several wastes cellulosic products such as shell flour, wood flour and pulp have also been used as reinforcing agents of different thermosetting and thermoplastic resins. It is well known that natural fibers impart high specific stiffness, strength and biodegradability to polymer matrix composites. Also, cellulosic fibers are readily available from natural sources and most importantly, they have low cost per unit volume.

There are many natural resources available which has potential to be applied in industries as raw materials such as pineapple, kenaf, coir, abaca, sisal, cotton, jute, bamboo, banana, Palmyra, talipot, hemp, and flex [1,2]. Among them Pineapple leaf fibre (PALF) is one of the waste materials in agriculture sector, which is widely grown in India as well as Asia. After banana and Citrus, Pineapple (Ananas comosus) is one of the most essential tropical fruits in the world [3]. Commercially pineapple leaves are considered as waste materials of fruit which is being used for producing natural fibers. The chemical composition of PALF constitute holocellulose (70– 82%), lignin (5–12%), and ash (1.1%).

Major constituents in a natural fiber reinforced composite are the reinforcing fibers and a matrix, which acts as a binder for the fibers. In addition, particulate fillers can also be used with some polymeric matrices primarily to reduce cost and improve their dimensional stability. So, although a judicious selection of matrix and the reinforcing phase can lead to a composite with a combination of strength and modulus comparable to or even better than those of conventional metallic materials [4], the physical and mechanical characteristics can further be modified by adding a solid filler phase to the matrix body during the composite preparation. The fillers play a major role in determining the properties and behaviour of particulate reinforced composites.

Production of alumina from bauxite by the Bayer's process is associated with the generation of red mud as the major waste material in alumina industries worldwide. Depending upon the quality of bauxite, the quantity of red mud generated varies from 55-65% of the bauxite processed. Detailed characterization of red mud generated from NALCO aluminium refinery at Damanjodi, India is reported by Mohapatra et al. [4]. To obtain the desired properties from a hybrid composite system, reinforcement and fillers are added to the polymers [5].

Another possibility that the incorporation of both particulates and fibers in polymer could provide a synergism in terms of improved properties and wear performance has not been adequately explored so far. However, some recent reports suggest that by incorporating filler particles into the matrix of fiber reinforced composites, synergistic effects may be achieved in the form of higher modulus and reduced material cost, yet accompanied with decreased strength and impact toughness. Such multi-component composites consisting of a matrix phase reinforced with a fiber and filled with particulates are termed as hybrid composites.

Nowadays much attention is devoted towards the study of solid particle erosion behaviour of polymer composites due to the high potential use of these materials in many mechanical and structural applications. Hence, erosion resistance of polymer composites has become an important material property, particularly in selection of alternative materials and therefore the study of solid particle erosion characteristics of the polymeric composites has become highly relevant. Differences in the erosion behaviour of various types of composite materials are caused by the Amount, Type, Orientation and Properties of the reinforcement on one hand and by the type and properties of the matrix and its adhesion to the fibers/fillers on the other hand. A full understanding of the effects of all system variables on the wear rate is necessary in order to undertake appropriate steps in the design of machine or structural component and in the choice of materials to reduce/control wear [6].

II. EXPERIMENTAL DETAILS

A. Materials:

In this present research work Vinylester is chosen as the matrix material, i.e. grade of FB-701, Density 1.35 gm/cc, Elastic modulus 3.25 Gpa, (Supplied by Zenith Industrial supplies, Bangalore) and the Raw natural Pineapple leaf fiber(PALF) mat is unidirectional horizontal. The width is 17 inch and thickness is 2.8 mm, Density 1.56 gm/cc, Elastic Modulus 62.1 Gpa, (supplied by Go-green products, Chennai) are used as the reinforcing phase in the composites.

Though the present research work is focused mainly on the pineapple leaf fiber reinforced composites, their relative evaluation can only be made on comparing them with a similar set of composites with some conventional synthetic fiber. In the present work, E-glass fibers chopped strand mat density 2.54 gm/cc; modulus 72.4 Gpa, (supplied by Zenith Industrial supplies, Bangalore) has been used as the reinforcing material in the composites. The major constituents of E-glass are silicon oxide (54 wt. %), aluminum oxide (15 wt. %), calcium oxide (17 wt. %), boron oxide (8 wt. %) and magnesium oxide (4.5 wt. %).

A variety of natural or synthetic solid particulates, both organic and inorganic is already being commercially used as reinforcing fillers in polymeric composites. While ceramic powders such as alumina (Al_2O_3), silicon carbide (SiC) , silica (SiO_2), titanium (TiO_2) etc. are widely used as conventional fillers, the use of industrial wastes for such purpose is hardly found. In view of this, in the present work an industrial waste such as Redmud are chosen as particulate fillers to be used in the composites. The red mud used in this work has been collected from the site of NALCO alumina plant at Damanjodi in India. The chemical compositions and density of Redmud particulate filler materials for this study are mentioned in the Table 1.

Table 1. Chemical compositions and density of Redmud filler materials

Filler	Composition/Chemical formula	Density (gm/cc)
Red mud	Fe_2O_3 (40%), Al_2O_3 (20%), SiO_2 (14%), Na_2O (6%), CaO (4%), TiO_2 (2%)	3.26

B. Composite Fabrication

The resin used in this research work is Vinylester FB-701 resin (density 1.35 gm/cc, Elastic modulus 3.25Gpa) and reinforcing phase a unidirectional Pineapple Leaves Fiber (PALF) and E-glass fibers are reinforced separately in Vinylester resin to prepare the fiber reinforced composites P_1 and G_1 in which no particulate filler Material is used. The other composite samples $P_2 – P_3$ and $G_2 – G_3$ with Redmud particulate fillers of varied amount but with fixed fiber loading (30 wt %) are fabricated. The composition and designation of the composites prepare for this study are listed in Table 2.

The fabrication of the composite slabs is done by conventional hand-lay-up technique followed by light compression moulding technique. The Cobalt Naphthenate 2% is mixed thoroughly in Vinylester resin and then 2% methyl ethyl ketone peroxide (MEKP), 2% N- dimethylaniline is mixed in the resins prior to reinforcement. The fiber loading weight fraction of unidirectional Pineapple Leaves Fiber (PALF) or E-glass fiber chopped strand mat in the composite is kept 30 wt% for all the

samples. The stacking procedure consists of placing the fabric one above the other with the resin mix well spread between the fabrics on a mould release sheet.

Table 2. Designations and detailed compositions of the composites

Designation	Composition
P_1	Vinylester (70 wt%) + PALF (30 wt%)
P_2	Vinylester (60 wt%) + PALF (30 wt%) + Red mud (10 wt%)
P_3	Vinylester (50 wt%) + PALF (30 wt%) + Red mud (20 wt%)
G_1	Vinylester (70 wt%) + Glass Fiber (30wt%)
G_2	Vinylester (60 wt%) + Glass Fiber (30wt%) + Red mud (10 wt%)
G_3	Vinyl ester (50 wt%) + Glass Fiber(30wt%) + Red mud (20 wt%)

A porous Teflon film was again used to complete the stack. To ensure uniform thickness of the sample, a 4mm spacer was used. The mould plates were coated with release agent in order to aid the ease of separation on curing. A metal roller was used so that uniform thickness and compactness could obtain The whole assembly is placed in the light compression molding machine at a pressure of 40Kgf/cm2 and allowed to cure at room temperature for 24hrs. The laminate sheets of sizes 210 x 210 x 4mm were prepared. Specimens of suitable dimensions were cut using a diamond cutter for physical and mechanical characterization as per ASTM standard.

C. Erosion Wear test

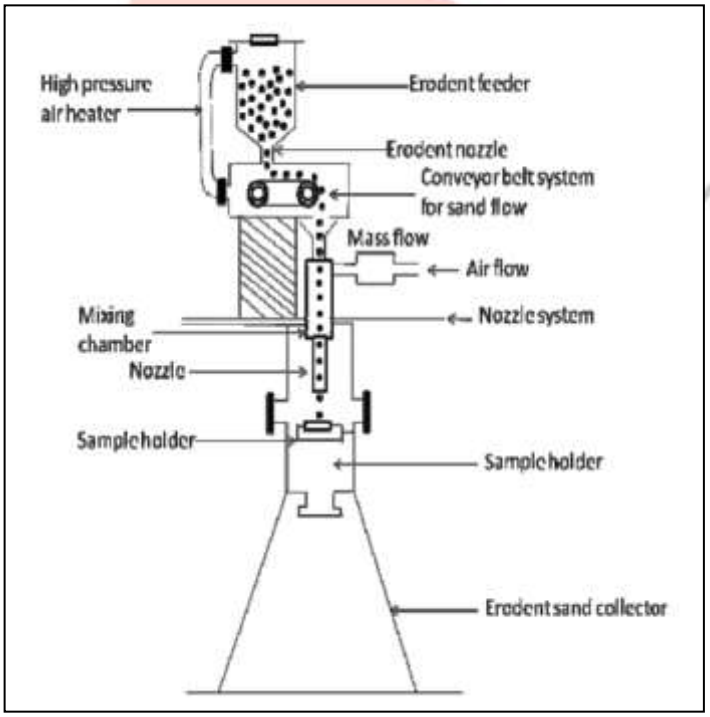

Figure 1. A Schematic Diagram of the Erosion Test Rig

The set up for the solid particle erosion wear test used in this study is capable of creating reproducible erosive situations for assessing erosion wear resistance of the prepared composite samples. The pictorial view and the schematic diagram of the erosion test rig are given in Figure 1. The test rig consists of an air compressor, an air drying unit, a conveyor belt-type particle feeder and an air particle mixing and accelerating chamber. In the present study, dry silica sand (assumed to be square pyramidal shaped) of different particle sizes (300µm, 450µm and 600µm) are used as the erodent. The dried and compressed air is mixed with the erodent which is fed constantly by a conveyor belt feeder into the mixing chamber and then is accelerated by passing the mixture through a convergent brass nozzle of 3 mm internal diameter. The erodent particles impact the specimen which can be held at different angles with respect to the direction of erodent flow using a swivel and an adjustable sample clip. The velocity of the eroding particles is determined using the standard double disc method. The apparatus is equipped with a heater which can regulate and maintain the erodent temperature at any pre-determined fixed value during an erosion trial. The samples are cleaned in

acetone, dried and weighed before and after the erosion trials using a precision electronic balance to an accuracy of ± 0.1 mg. The weight loss is recorded for subsequent calculation of erosion rate. The process is repeated till the erosion rate attains a constant value called steady state erosion rate. The erosion rate is defined as the ratio of this weight loss to the weight of the eroding particles causing the loss

D. Taguchi Method

In any experimental research, since test procedures are generally expensive and time consuming, the need to satisfy the design objectives with the least number of tests is clearly an important requirement. In this context, Taguchi method provides the designer with a systematic and efficient approach for experimentation to determine near optimum settings of design parameters for performance and cost. This method involves laying out the experimental conditions using specially constructed tables known as 'orthogonal arrays'. Use of orthogonal arrays significantly reduces the number of experimental configurations to be studied. The conclusions drawn from small scale experiments are valid over the entire experimental region spanned by the control factors and their settings. The most important stage in the design of experiment lies in the selection of the control factors. Therefore, initially a large number of factors are included so that non-significant variables can be excluded at the earliest opportunity. Exhaustive literature review reveals that parameters i.e. impact velocity, impingement angle; fiber loading, filler content, erodent size, stand-off distance etc. largely influence the erosion rate of polymer composites [6, 7].

However, the author has not come across any report on the influence of a factor like erodent temperature on wear performance of polymer composites. Therefore, the present work, to explore the possible effect of erodent temperature, it is also considered as a control factor in addition to impact velocity, impingement angle, filler content, erodent size and stand-off distance. Thus, the impact of six parameters are studied using L_{27} (3^{13}) orthogonal design. The control factors and the parameter settings for erosion test are given in Table 3. and Table 4. presents the selected levels for various control factors.

The standard linear graph as shown in Figure 2. is used to assign the factors and interactions to various columns of the orthogonal array [8]. The selected parameters viz., impact velocity, filler content, erodent temperature, stand-off distance, impingement angle and erodent size, each at three levels, are considered in this study. These six parameters each at three levels would require $3^6 = 729$ runs in a full factorial experiment whereas Taguchi's experimental approach reduces it to 27 runs only offering a great advantage.

Table 3. Parameter settings for erosion test

Control Factors	**Symbols**	**Fixed parameters**	
Impact velocity	Factor A	Erodent	Silica sand
Filler content	Factor B	Erodent feed rate (g/min)	10.0 +1.0
Erodent Temperature	Factor C	Nozzle diameter (mm)	3
Impingement angle	Factor D	Length of nozzle (mm)	80
Standoff distance	Factor E		
Erodent size	Factor F		

Table 4. Levels for various control factors

Control factor	**LEVEL**			**Unit**
	I	**II**	**III**	
A: Impact velocity	45	55	65	m/sec
B: Filler content	0	10	20	%
C:Erodent Temperature	40	50	60	°C
D: Impingement angle	30	60	90	degree
E: Stand-off distance	65	75	85	mm
F: Erodent size	300	450	600	μm

The plan of the experiments as shown in Table 5. is as follows: the first, second, fifth, ninth, tenth and twelfth columns are assigned to impact velocity (A), filler content (B), erodent temperature (C), impingement angle (D), stand-off distance (E) and erodent size (F) respectively. The third and fourth column are assigned to $(AXB)_1$ and $(AXB)_2$ respectively to estimate interaction between impact velocity (A) and filler content (B), the sixth and seventh column are assigned to $(BXC)_1$ and $(BXC)_2$ respectively to estimate interaction between filler content (B) and erodent temperature (C), the eighth and eleventh column are assigned to $(AXC)_1$ and $(AXC)_2$ respectively to estimate interaction between the impact velocity (A) and erodent temperature (C) and the remaining columns are used to estimate experimental errors.

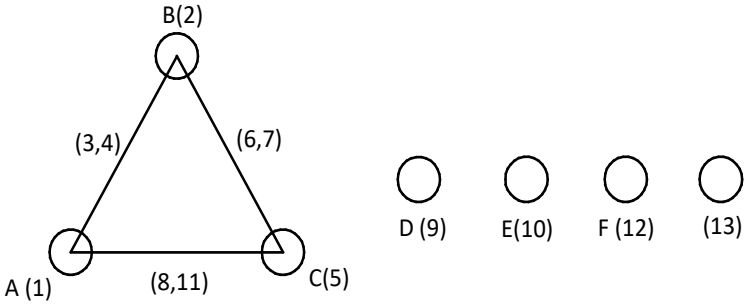

Figure 2. Linear graphs for L_{27} orthogonal array

Table 5. Orthogonal array for L_{27} (3^{13}) Taguchi Design

L_{27} (3^{13})	1 A	2 B	3 $(AxB)_1$	4 $(AxB)_2$	5 C	6 $(BxC)_1$	7 $(BxC)_2$	8 $(AxC)_1$	9 D	10 E	11 $(AxC)_2$	12 F	13
1	1	1	1	1	1	1	1	1	1	1	1	1	1
2	1	1	1	1	2	2	2	2	2	2	2	2	2
3	1	1	1	1	3	3	3	3	3	3	3	3	3
4	1	2	2	2	1	1	1	2	2	2	3	3	3
5	1	2	2	2	2	2	2	3	3	3	1	1	1
6	1	2	2	2	3	3	3	1	1	1	2	2	2
7	1	3	3	3	1	1	1	3	3	3	2	2	2
8	1	3	3	3	2	2	2	1	1	1	3	3	3
9	1	3	3	3	3	3	3	2	2	2	1	1	1
10	2	1	2	3	1	2	3	1	2	3	1	2	3
11	2	1	2	3	2	3	1	2	3	1	2	3	1
12	2	1	2	3	3	1	2	3	1	2	3	1	2
13	2	2	3	1	1	2	3	2	3	1	3	1	2
14	2	2	3	1	2	3	1	3	1	2	1	2	3
15	2	2	3	1	3	1	2	1	2	3	2	3	1
16	2	3	1	2	1	2	3	3	1	2	2	3	1
17	2	3	1	2	2	3	1	1	2	3	3	1	2
18	2	3	1	2	3	1	2	2	3	1	1	3	2
19	3	1	3	2	1	3	2	1	3	2	1	3	2
20	3	1	3	2	2	1	3	2	1	3	2	1	3
21	3	1	3	2	3	2	1	3	2	1	3	2	1
22	3	2	1	3	1	3	2	2	1	3	3	2	1
23	3	2	1	3	2	1	3	3	2	1	1	3	2
24	3	2	1	3	3	2	1	1	3	2	2	1	3
25	3	3	2	1	1	3	2	3	2	1	2	1	3
26	3	3	2	1	2	1	3	1	3	2	3	2	1
27	3	3	2	1	3	2	1	2	1	3	1	3	2

The experimental observations are transformed into signal-to-noise (S/N) ratios. There are several S/N ratios available depending on the type of characteristics such as:

$$'\text{Smaller} - \text{the} - \text{better}' \text{ characterstic}:$$

$$\frac{S}{N} = -10 \log \frac{1}{n}\left(\sum y^2\right) \qquad (1)$$

Where **n** is the number of observations, **y** is the observed data, **Y** the mean and **S** the variance. The S/N ratio for minimum erosion rate comes under 'smaller-the-better' characteristic, which can be calculated as logarithmic transformation of the loss function by using Eq. (1).

III. RESULT AND DISCUSSION

A. Erosion Wear Characteristics

This part presents the analysis and comparison of erosion response of PALF-Vinylester and Glass-Vinylester composites filled with Redmud. The experiments have been carried out using Taguchi experimental design (L_{27} Orthogonal array) given in Table 5. and the subsequent analysis of the test results is made using the popular software specifically used for design of experiment applications known as MINITAB 18. Finally, the micro-structural features of the composite samples eroded under different operating conditions are described based on SEM micrographs.

B. Taguchi Experimental Analysis

The results of erosion experiments carried out according to Taguchi experimental design on Red mud filled PALF-Vinylester and Glass-Vinylester composites, the overall mean of the S/N ratios is found to be -46.5774 db for PALF based composites and -47.5443 db for the Glass based ones. For similar test conditions, PALF-Vinylester composites exhibit much lower wear rates than those by Glass-Vinylester composites.

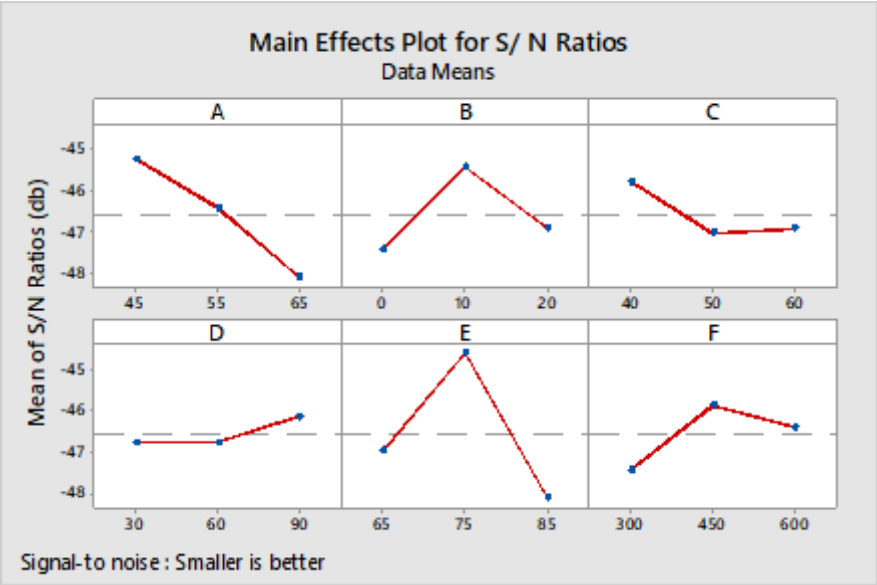

*A= Impact Velocity, B=Filler content, C= Erodent Temperature, D=Impingement angle, E= Stand –off-distance, F=Erodent Size

Figure 3. Effect of control factors on erosion rate (For Red mud filled PALF-Vinylester composites)

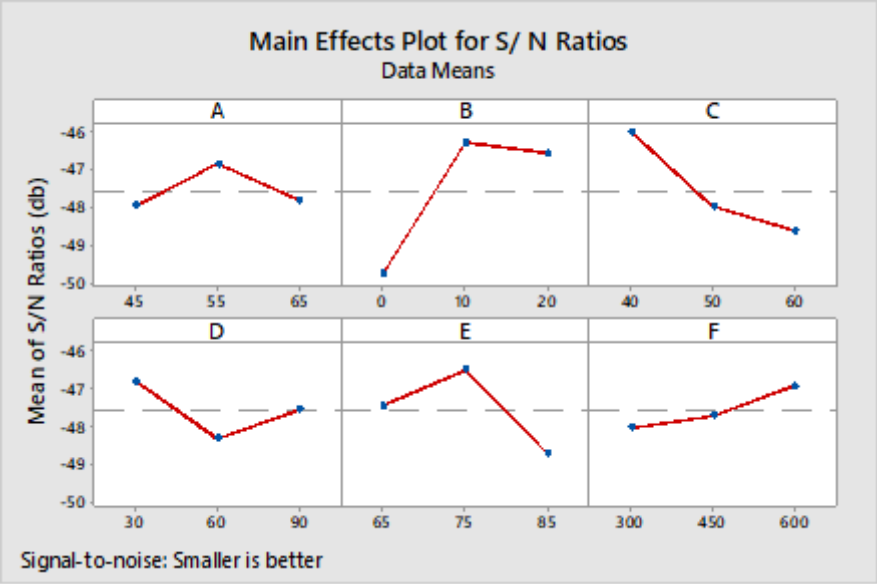

*A= Impact Velocity, B=Filler content, C= Erodent Temperature, D=Impingement angle, E= Stand –off-distance, F=Erodent Size

Figure 4. Effect of control factors on erosion rate (For Red mud filled Glass-Vinylester composites)

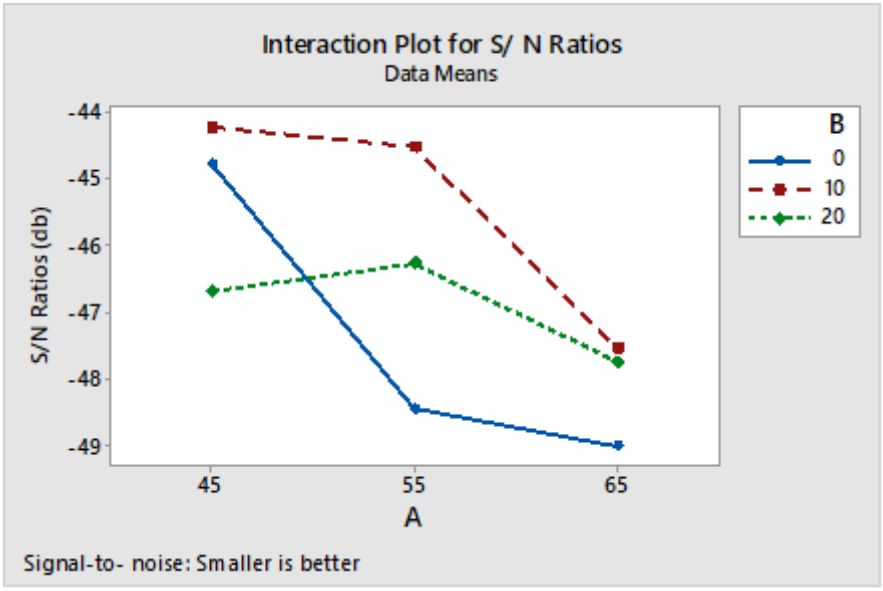

*A= Impact Velocity, B=Filler content

Figure 5. Interaction graph between impact velocity and filler content (A X B) for erosion rate (For Red mud filled PALF-Vinylester composites)

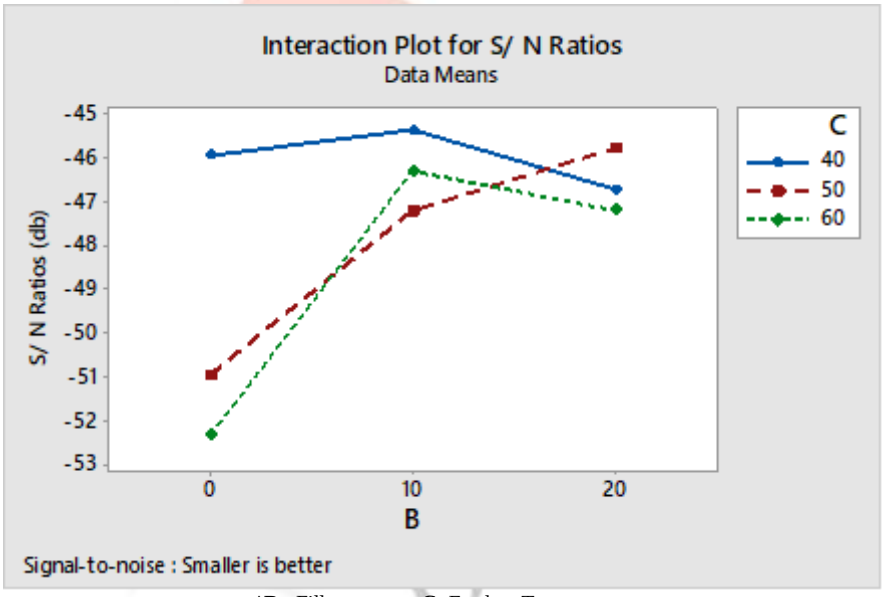

*B= Filler content, C=Erodent Temperature

Figure 6. Interaction graph between filler content and erodent temperature (B X C) for erosion rate (For Red mud filled Glass- Vinylester composites)

Figures 3. and Figure 4. illustrate the effect of control factors on erosion rate of PALF-Vinylester and Glass-Vinylester composites respectively. Analysis of the results leads to the conclusion that factor combination of A1(Impact velocity: 45 m/sec), B2 (Filler content: 10wt%), C1(Erodent temperature: 40^0C), D3 (Impingement angle: 90^0), E2 (Stand-off distance: 75mm) and F2 (Erodent size: 450µm) gives minimum erosion rate (Figure 3) for PALF-Vinylester composites and the factor combination of A2 (Impact velocity: 55 m/sec), B2 (Filler content: 10wt%), C1(Erodent temperature: 40^0C), D1 (Impingement angle: 30^0), E2 (Stand-off distance: 75mm) and F3 (Erodent size: 600µm) gives minimum erosion rate (Figure 4) for Glass-Vinylester composites. The respective interaction graphs are shown in the Figures 5. and Figure 6. for PALF-Vinylester and Glass-Vinylester composites respectively.

C. ANOVA and the Effects of Factors

Table 6. and Table 7. show the results of the ANOVA for the erosion rate of PALF-Vinylester composites and Glass - Vinylester composites respectively. The last column of the table indicates percentage contribution of the control factors and their interactions on the performance output i.e. erosion rate [9].

From Table 6. It can be observed for the Red mud filled PALF-Vinylester composites that stand-off distance (p=0.342), impact velocity (p = 0.450), filler content (p = 0.614), erodent size (p= 0.725) and erodent temperature (p=0.782) have considerable influence on erosion rate. The interaction of impact velocity and red mud content (p=0.861) as well as Red mud content and erodent temperature (p=0.864) show significant contribution on the erosion rate but the remaining factors and interactions have relatively less significant contribution on erosion rate.

Similarly, from Table 7. It can be observed for the red mud filled Vinylester composites with glass reinforcement that red mud content (p=0.009), erodent temperature (p = 0.017), stand-off distance (p = 0.026), impingement angle (p= 0.053) and impact velocity (p=0.083) have great influence on erosion rate. The interaction of impact velocity and red mud content (p=0.018) as well as red mud content and erodent temperature (p=0.027) show significant contribution on the erosion rate but the remaining factors and interactions have relatively less significant contribution on erosion rate.

Table 6. ANOVA table for erosion rate (For Red mud filled PALF-Vinylester composites)

Source	DF	Seq SS	Adj SS	Adj MS	F-Value	P-Value
A	2	37.389	37.389	18.695	1.22	0.450
B	2	19.239	19.239	9.620	0.63	0.614
C	2	8.538	8.538	4.269	0.28	0.782
D	2	2.447	2.447	1.224	0.08	0.926
E	2	58.736	58.736	29.368	1.92	0.342
F	2	11.590	11.590	5.795	0.38	0.725
A X B	4	18.175	18.175	4.544	0.30	0.861
A X C	4	10.750	10.750	2.688	0.18	0.932
B X C	4	17.849	17.849	4.462	0.29	0.864
Error	2	30.595	30.595	15.298		
Total	26	215.309				

***DF**: Degree of Freedom, **Seq SS**: Sequential sum of squares, **Adj.SS**: Extra sum of squares, **Seq MS**: Sequential mean square, **F-Value**: F-test, **P-Value**: Percent Contribution

Table 7. ANOVA table for erosion rate (For Red mud filled Glass-Vinylester composites)

Source	DF	Seq SS	Adj SS	Adj MS	F-Value	P-Value
A	2	6.518	6.518	3.2588	11.08	0.083
B	2	66.358	66.358	33.1790	112.85	0.009
C	2	33.123	33.123	16.5615	56.33	0.017
D	2	10.489	10.489	5.2444	17.84	0.053
E	2	21.822	21.822	10.9112	37.11	0.026
F	2	5.947	5.947	2.9735	10.11	0.090
A X B	4	66.073	66.073	16.5182	56.18	0.018
A X C	4	7.081	7.081	1.7703	6.02	0.147
B X C	4	43.042	43.042	10.7604	36.60	0.027
Error	2	0.588	0.588	0.2940		
Total	26	261.040				

***DF**: Degree of Freedom, **Seq SS**: Sequential sum of squares, **Adj.SS**: Extra sum of squares, **Seq MS**: Sequential mean square, **F-Value**: F-test, **P-Value**: Percent Contribution

D. Confirmation Experiment

The confirmation experiment is performed by taking an arbitrary set of factor combination $A_2B_3C_2E_1F_3$. Here, factor D has been omitted for being the least significant. Similarly, for Glass-Vinylester composites the arbitrary set of factor combination $A_3B_3C_2D_3E_1$ is taken. Factor F has been omitted since it has least effect on performance characteristics. The estimated S/N ratio for erosion rate can be calculated with the help of following prediction equation:

$$\bar{\eta}_{\text{PALF-Red mud}} = \bar{T} + (\bar{A}_2 - \bar{T}) + (\bar{B}_3 - \bar{T}) + [(\bar{A}_2\bar{B}_3 - \bar{T}) - (\bar{A}_2 - \bar{T}) - (\bar{B}_3 - \bar{T})] + (\bar{C}_2 - \bar{T}) + [(\bar{B}_3\bar{C}_2 - \bar{T}) - (\bar{B}_3 - \bar{T}) - (\bar{C}_2 - \bar{T})] + (\bar{E}_1 - \bar{T})(\bar{F}_3 - \bar{T}) \quad (2)$$

$$\bar{\eta}_{\text{GF-Red mud}} = \bar{T} + (\bar{A}_3 - \bar{T}) + (\bar{B}_3 - \bar{T}) + [(\bar{A}_3\bar{B}_3 - \bar{T}) - (\bar{A}_3 - \bar{T}) - (\bar{B}_3 - \bar{T})] + (\bar{C}_2 - \bar{T}) + [(\bar{B}_3\bar{C}_2 - \bar{T}) - (\bar{B}_3 - \bar{T}) - (\bar{C}_2 - \bar{T})] + (\bar{D}_3 - \bar{T}) + (\bar{E}_1 - \bar{T}) \quad (3)$$

$\bar{\eta}_{\text{PALF-Red mud}}$ and $\bar{\eta}_{\text{GF-Red mud}}$: Predictive average for Flyash filled PALF fiber based and Glass fiber based composites respectively.

$\overline{T}$ = Overall experimental average

$\overline{A}_2, \overline{A}_3, \overline{B}_3, \overline{C}_2, \overline{C}_3, \overline{D}_3, \overline{E}_1$, and $\overline{F}_3$: Mean Response for Factor and Interactions at designated levels.

By combining like terms, the Equation (2) and Equation (3) reduces to

$$\overline{\eta}_{\text{PALF-Red mud}} = \overline{A}_2\overline{B}_3 + \overline{B}_3\overline{C}_2 - \overline{B}_3 + \overline{E}_1 + \overline{F}_3 - 2\overline{T} \quad (4)$$

$$\overline{\eta}_{\text{GF-Red mud}} = \overline{A}_3\overline{B}_3 + \overline{B}_3\overline{C}_2 - \overline{B}_3 + \overline{D}_3 + \overline{E}_1 - 2\overline{T} \quad (5)$$

A new combination of factor levels A_2, B_3, B_2, C_2,C_3, D_3, E_1, and F_3 is used to predict erosion rate through prediction equation and it is found to be $\overline{\eta}_{\text{PALF-Red mud}}$ = - 47.9582 dB and $\overline{\eta}_{\text{GF-Red mud}}$= - 47.8792 dB respectively.

For each performance measure, an experiment is conducted for the same set of factor combinations and the obtained S/N ratio value is compared with that obtained from the predictive equation as shown in Table 8. The resulting model seems to be capable of predicting erosion rate to a reasonable accuracy. An error of 4.62 % and 3.60 % for the S/N ratio of erosion rate is observed for PALF-Vinylester composites and Glass-Vinylester composites respectively. However, the error can be further reduced if the number of measurements is increased. This validates the mathematical model for predicting the measures of performance based on knowledge of the input parameters.

Table 8. Results of the confirmation experiments for erosion rate

	Optimal control parameters (For PALF-Vinylester composites)		Optimal control parameters (For Glass-Vinylester composites)	
	Prediction	Experimental	Prediction	Experimental
Level	$A_2B_3C_2E_1F_3$	$A_2B_3C_2E_1F_3$	$A_3B_3C_2D_3E_1$	$A_3B_3C_2D_3E_1$
S/N ratio for Erosion rate(db)	-47.9582	-45.7412	-47.8792	-46.1532

E. Effect of Impingement Angle and Erodent Temperature on Erosion

The variation of erosion rate of the red mud filled PALF-Vinylester and Glass-Vinylester composites with impingement angle is obtained by conducting experiments under specified operating conditions (Figure 7.). It shows the peak erosion taking place at an impingement angle of 60^0 for the unfilled as well as for the red mud filled PALF-Vinylester and Glass-Vinylester composites. This clearly indicates that these composites respond to solid particle impact neither in a purely ductile nor in a purely brittle manner. This behaviour can be termed as semi-ductile in nature which is in agreement with the trend observed in previous investigations [10].

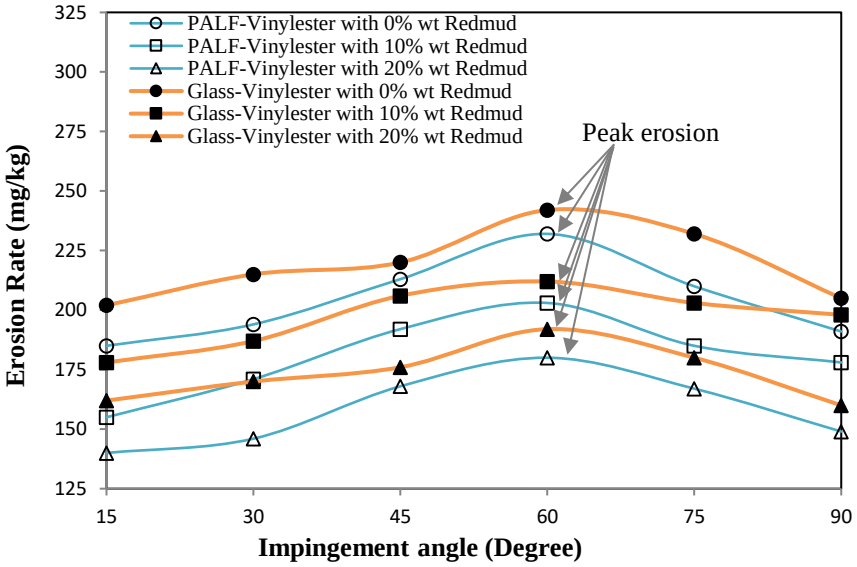

Figure 7. Effect of impingement angle on the erosion wear rate of Redmud filled composites

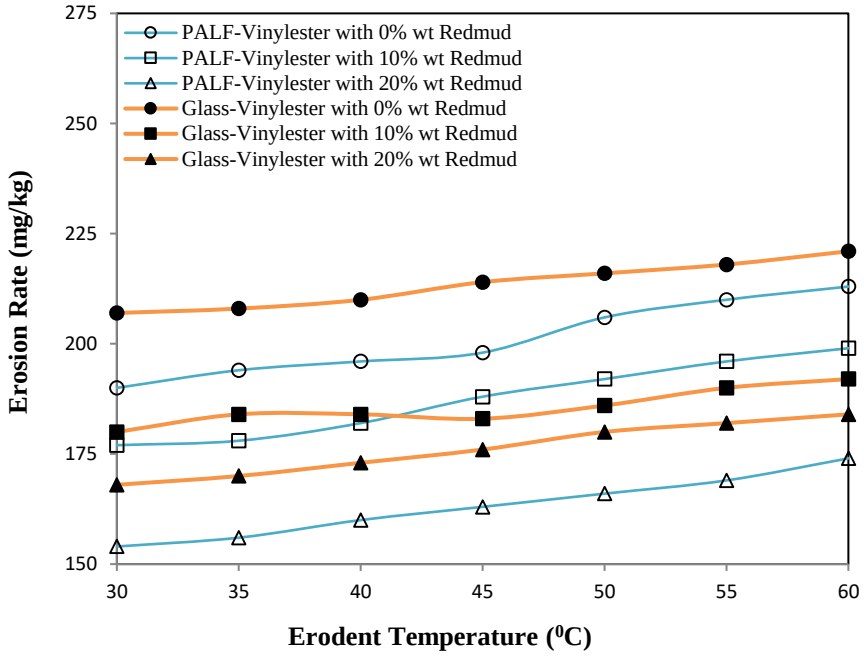

Figure 8. Effect of erodent temperature on the erosion wear rate of Redmud filled composites

Similarly, erosion trials are conducted at seven different erodent temperatures under normal impact condition and the variation of erosion rate of unfilled and red mud filled composites with erodent temperature is shown in Figure 8. It is evident from the figure that for all the composite samples, the erosion rates remain almost unaffected by the change in erodent temperature from ambient to 40^0C. However, the effect of erodent temperature on erosion rate is significant above 40^0C and the rate of increase in erosion rate is greater at higher erodent temperatures. The increase in erosion rate with erodent temperature can be attributed to increased penetration of particles on impact as a result of dissipation of greater amount of particle thermal energy to the target surface. This leads to surface damage, enhanced crack growth and consequently to the reduction in erosion resistance.

F. Surface Morphology

To ascertain the wear mechanism in composites, scanning electron microscopy (SEM) has been done and the micrographs of the surfaces of unfilled and red mud filled composites eroded at different impingement angles are shown in Figures 9. and Figure 10. respectively. Figure 9. presents the SEM of the unfilled Redmud PALF-Vinylester composite surfaces eroded under various test conditions. In Figure 9(a), no cracks or craters are seen on the composite surface after erosion due to impact of dry silica sand particles (temperature 40^0C) of smallest erodent size (300 μm) with a lower impact velocity (45 m/sec) at an impingement angle of 90^0. But as the erosion tests are carried out at higher erodent temperature (60^0C) and erodent size (450 μm), the morphology of the eroded surface becomes different as in Figure 9 (b).

Generally, in ductile erosion response, repeated impacts lead to plastic indentation and heavily strained regions on the surface while in the case of brittle response, the propagation of cracks towards the surface and their intersection to form a wear particle separated from the surface lead to material loss. As seen in Figure 9 (a), both processes appear to be operative. Initially the surface is strained and displaced in the plane by repeated impacts of the erodent particles. Regions are formed due to simultaneous generation of cracks exhibiting a brittle response. The extent of plastic indentation, however, decreased as the angle of impingement is lowered as seen in other micrographs in Figures 9 (b-f). When the impingement angle is changed to 60^0, the features seen are quite different in Figure 9 (b). The normal component of the impact force was still effective in producing plastic indentation creating patches similar to Figure 9 (a). The tangential component, on other hand is now operative in cutting action. Most parts of the micrograph show evidence of material flow in the direction of impingement. As seen in Figures 9 (c), (d) and (e) with impact velocity of 65 m/sec and at an erodent temperature of 60^0C, the dominance of plastic indentation reduce with impingement angle, though micro-cracking persists. Figure 9 (f) shows unique features as the entire surface indicates the dominance of the micro-cutting process, a characteristic failure feature for ductile materials at very low angle. This mechanism is responsible for the highest material removal at an erodent temperature of 50^0C and impact velocity of 55m/sec. It is also evident from these microstructures that for higher erodent temperature and impact velocity, the damage to the surface is also relatively greater.

Morphologies of the worn surfaces of red mud filled PALF-Vinylester composites are shown in Figure 10. The removal of matrix material from the impact surface of the composite with 10wt % of red mud eroded at lower impingement angle (30^0), lower impact velocity (45m/sec) resulting in exposure of small amount of fibers to erosive environment can be clearly seen in Figure 10(a). The fibers are still held firmly in place as yet by the matrix surrounding them seen in Figure 10(b). The fiber matrix de-bonding, brittle fracture of matrix and pulverization of fibers are also reflected in the micrograph seen in Figure10 (b). When

impact velocity increases to 55m/sec, impingement angle changes to 60^0, erodent temperature at 60^0C and filler content 20wt%, the fibers are completely broken by means of shearing action and protruding of fibers from matrix are seen in Figures 10(c) and Figure (d).

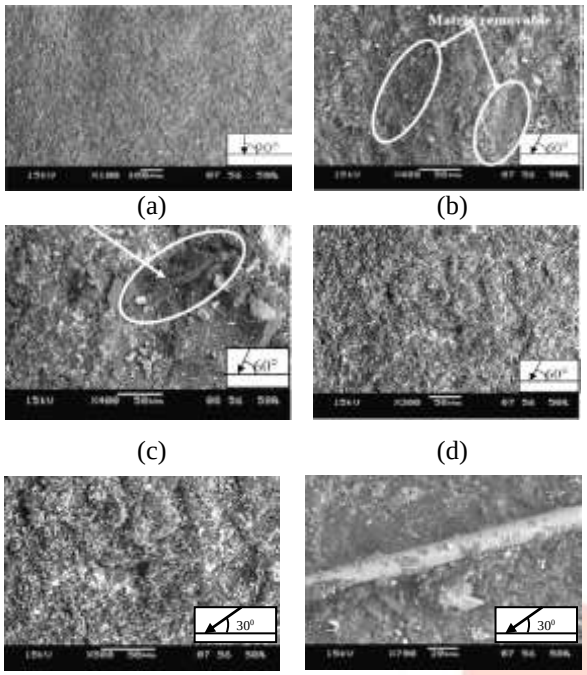

(a) (b)

(c) (d)

(e) (f)

Figure 9. SEM graph of eroded unfilled PALF -Vinylester composites

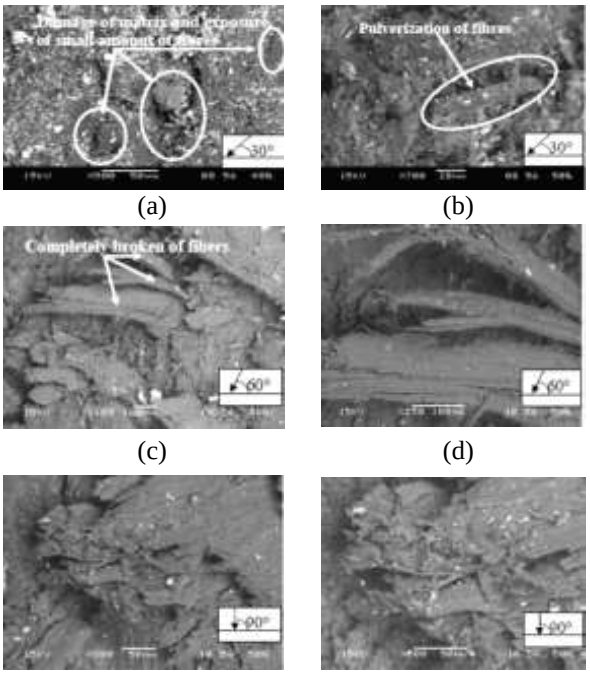

(a) (b)

(c) (d)

(e) (f)

Figure 10. SEM micrographs of the eroded PALF-Vinylester composites filled with Red mud

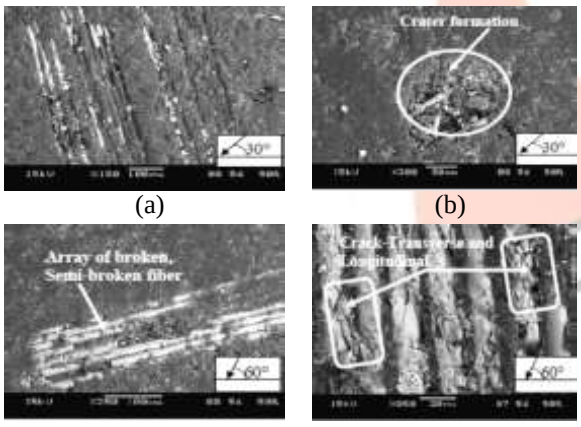

(a) (b)

(c) (d)

Figure 11. SEM graph of eroded unfilled PALF -Vinylester composites

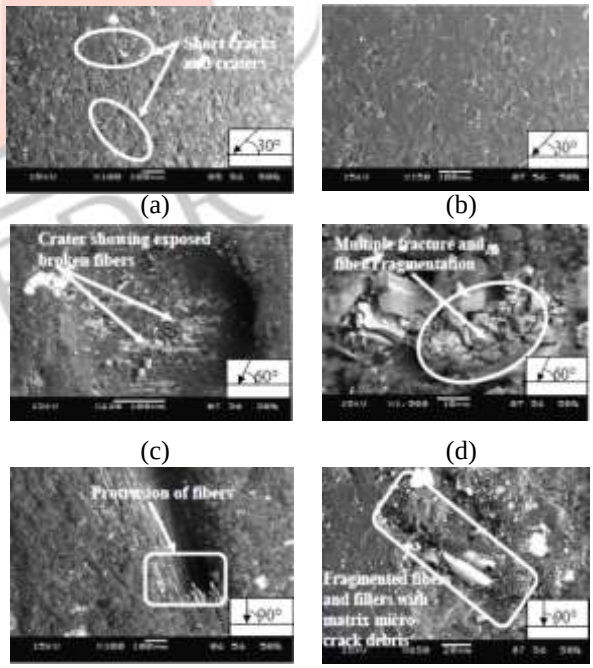

(a) (b)

(c) (d)

(e) (f)

Figure 12. SEM micrographs of the eroded PALF-Vinylester composites filled with Red mud

Figures 10(e) and Figure 10(f) show worn surfaces of PALF-Vinylester composite with 20 wt% red mud at higher impact velocity (65m/sec), higher impingement angle (90^0) and higher erodent temperature (60^0C). Here, the erosion mechanism is characterized by clean removal of the matrix and exposure of PALF fibers. Further damage is characterized by separation and detachment of broken fibers from the resin matrix. There is an evidence of fiber removal leaving behind cavities along the length of fibers seen in Figure 10(e). At higher impact velocity (65m/sec) due to continuous exposure of fibers to erosion environment results in fiber thinning, detachment of fibers from the matrix and cavities left after fiber being dislodged may also be seen in

Figure 10(f). Micro-cracking, micro-cutting and pulverization of matrix and fibers appear to be the main features in the micrograph. The damage at higher impact velocity is more severe, because of excessive wear and the fibers seem to be washed away from the surface seen in Figures 10 (c-f).

The magnitude of erosion rates caused by sand particle impact in PALF-Vinylester composites is found to be different from that in case of Glass-Vinylester composites although the same filler material i.e. red mud is present in both. So, in an attempt to get an insight to the material removal mechanism in these composites, SEM study of some of the eroded samples of Glass-Vinylester composites is also done.

Figure 11. Presents the SEM of surfaces of the unfilled Glass-Vinylester composite eroded under various test conditions. In Figure 6.11(a) the matrix is chipped off and the glass fibers are clearly visible beneath the matrix layer after the impact of dry silica sand particles (temperature 40^0C) of size (300 μm) with a lower impact velocity (45m/sec) at a low impingement angle of 30^0. The micrograph with a higher magnification presented in Figure 11(b) distinctly illustrates a crater formed due to material loss and the arrays of broken and semi-broken glass fibers within. Due to repeated impact of hard and high temperature sand particles there is initiation of cracks on the fibers and as erosion progresses, these cracks subsequently propagate on the fiber bodies both in transverse as well as in longitudinal manner. But when the erosion tests are carried out with higher erodent temperature (60^0C), impingement angle of 60^0 and erodent size (450 μm), the morphology of the eroded surface is different as shown in Figures 11(c) and Figure 11(d).

From the SEM observations of the eroded surfaces of the glass-Vinylester composites filled with different red mud content as shown in Figure 12. it appears that composites under consideration exhibit several stages of erosion and material removal process. Very small craters and short cracks are seen on the eroded surface of the composite with 10 wt% red mud indicating the initiation of matrix material loss from the surface in Figure 12(a). Figures 12(a) and Figure 12(b) also show signs of plastic deformation of the matrix material and when impacting at a low angle (30^0), the hard erodent particles penetrate the surface and cause material removal mostly by micro-ploughing. Figure 12(c) shows the micrograph of the same composite surface eroded at an impingement angle of 60^0 and an impact velocity of 55 m/sec. The matrix covering the fiber seems to be chipped off and the crater thus formed shows the fiber body which is almost intact. Repeated impact of the erodent has caused roughening of the surface. Fragmentation of the fibers as a result of cracks and multiple fractures are also distinctly shown in Figure 12(d).

Figures 12 (e-f) are the SEM images for the Glass-Vinylester composites filled with 20 wt% red mud. After the local removal of matrix, the arrays of fibers are normally exposed to erosive environment and subsequently the material removal becomes faster. The wear trace is distinctly visible and there is protrusion of fibers beneath the matrix layer as seen in Figure 12(e). The broken fiber and fragmented red mud particles, seen in Figure 12(f), are mixed with the matrix micro-flake debris and the damage of the composite is characterized by the separation and detachment of this debris.

IV. CONCLUSION

1. This study reveals the semi-ductile response for most of these particulate filled PALF/Glass Vinylester composites with respect to erosion wear. The peak erosion rate is found to be occurring at 60^0 impingement angle for the unfilled composites as well as for Red mud filled composites with both PALF as well as glass reinforcement.

2. The presence of particulate fillers in PALF- Vinylester composites improves their erosion wear resistance and this improvement depends on the type and content of the fillers. It is interesting to note that Red mud in spite of being industrial waste, show lower erosion rates. Further, the filler materials considered in this study, Red mud emerges as the best filler material to be used in Vinylester based composites, irrespective of fiber type, as far as the resistance to solid particle erosion is concerned.

V. ACKNOWLEDGMENT

The authors gratefully acknowledge the facilities provided by M/s Texpertech Insulation, Hebbal industrial area, Mysuru, India, for the successful completion of fabrication Process to making the components. The Author thankful to National Institute of Engineering, Mysuru, facilities provided for successful completion of experimental work on Erosion Test Rig. And also author thankful to National Aluminium Co. (NALCO) located at Damanjodi in India for providing Redmud wastage material to preparing component.

REFERENCES

[1] R.M. Rowell, A. R. Sanadi, D. F. Caulfield, and R. E. Jacobson, ―Utilization of natural fibres in plastic composites-problems and opportunities, in *Lignocellulosic-Plastics Composites*, 1997.
[2] L. Yan, N. Chouw, and K. Jayaraman, ―Flax fibre and its composites—a review, *Composites Part B: Engineering*, vol. 56, pp. 296–317, 2014.
[3] R. M. N. Arib, S. M. Sapuan, M. A. M.M. Hamdan, M. T. Paridah, and H. M. D. K. Zaman, ―A literature review of pineapple fibre reinforced polymer composites, *Polymers and Polymer Composites*, vol. 12, no. 4, pp. 341–348, 2004.
[4] B. K. Mahapatra, M. B. S. Rao, R BhimaRao, A. K. Paul "Characteristics of Red Mud Generated at NALCO Refinery, Damanjodi, India," Ligh. Met., 2002, pp. 161–165.

[5] Jang B. Z, (1994). Advanced Polymer composites; Principles and Applications, ASM International.
[6] Thomas H. Kosel, (1992). Solid Particle Erosion, ASM Handbook, ASM International, 18, 199 213. (T.H. Kosel. In: P.J. Blau, Editor, Friction, Lubrication and Wear Technology, ASM Handbook, 18, pp. 207).
[7] Patnaik A, Satapathy A, Mahapatra S. S and Dash R. R, (2008). A Modeling Approach for Prediction of Erosion Behaviour of Glass Fiber- Polyester Composites, Journal of Polymer Research, 15(2), pp. 147-160.
[8] Patnaik A, Satapathy A, Mahapatra S. S and Dash R. R, (2009). Tribo- Performance of Polyester Hybrid Composites: Damage Assessment and Parameter Optimization using Taguchi Design, Materials and Design, 30(1), pp. 57-67.
[9] Phadke M. S, (1989). Quality Engineering using Robust Design, Prentice-Hall, Englewood Cliffs, NJ.
[10] Montgomery D. C, (2005). Design and Analysis of Experiments, Fifth Ed. John Wiley & Sons, Inc. pp. 363-382.
[11] Roy M, Vishwanathan B and Sundararajan G, (1994). Solid particle erosion of polymer matrix composites, Wear, 171(1-2), pp. 149-161.